# Epithelial Sel1L is required for the maintenance of intestinal homeostasis

Shengyi Sun[a,b,*], Rohan Lourie[c], Sara B. Cohen[d], Yewei Ji[a], Julia K. Goodrich[e], Angela C. Poole[f,g], Ruth E. Ley[e,f,g], Eric Y. Denkers[d], Michael A. McGuckin[c], Qiaoming Long[h], Gerald E. Duhamel[i], Kenneth W. Simpson[j], and Ling Qi[a,b]

[a]Division of Nutritional Sciences, [b]Graduate Program in Biochemistry, Molecular and Cell Biology, [e]Graduate Program in Genetics, Genomics and Development, [f]Department of Microbiology, and [g]Department of Molecular Biology and Genetics, Cornell University, Ithaca, NY 14853; [c]Immunity, Infection and Inflammation Program, Mater Medical Research Institute, Mater Health Services, South Brisbane, Queensland 4101, Australia; [d]Department of Microbiology and Immunology, [i]Department of Biomedical Sciences, and [j]Department of Clinical Science, College of Veterinary Medicine, Cornell University, Ithaca, NY 14853; [h]Laboratory Animal Research Center, Medical College of Soochow University, Suzhou 215006, Jiangsu, China

**ABSTRACT** **Inflammatory bowel disease (IBD) is an incurable chronic idiopathic disease that drastically decreases quality of life. Endoplasmic reticulum (ER)–associated degradation (ERAD) is responsible for the clearance of misfolded proteins; however, its role in disease pathogenesis remains largely unexplored. Here we show that the expression of SEL1L and HRD1, the most conserved branch of mammalian ERAD, is significantly reduced in ileal Crohn's disease (CD). Consistent with this observation, laboratory mice with enterocyte-specific Sel1L deficiency (*Sel1L*$^{\Delta IEC}$) develop spontaneous enteritis and have increased susceptibility to *Toxoplasma gondii*–induced ileitis. This is associated with profound defects in Paneth cells and a disproportionate increase of *Ruminococcus gnavus*, a mucolytic bacterium with known association with CD. Surprisingly, whereas both ER stress sensor IRE1α and effector CHOP are activated in the small intestine of *Sel1L*$^{\Delta IEC}$ mice, they are not solely responsible for ERAD deficiency–associated lesions seen in the small intestine. Thus our study points to a constitutive role of Sel1L-Hrd1 ERAD in epithelial cell biology and the pathogenesis of intestinal inflammation in CD.**

**Monitoring Editor**
Reid Gilmore
University of Massachusetts

Received: Oct 20, 2015
Revised: Nov 23, 2015
Accepted: Nov 23, 2015

## INTRODUCTION

Inflammatory bowel disease (IBD) is a devastating disease that affects millions of people worldwide. Phenotypically, IBD is categorized as Crohn's disease (CD), which is defined by transmural inflammation of the ileum and or colon, or ulcerative colitis (UC), which is a mucosal inflammation and ulceration restricted to the colon. The etiology of IBD is unresolved, but it is generally considered as a disturbed host–microbial symbiosis in a genetically susceptible individual, leading to aberrant proinflammatory immune responses (Wlodarska *et al.*, 2015). The intestinal epithelium is the physical interface between the host and gut microbiota. Absorptive enterocytes and specialized cells such as Paneth and goblet cells, which actively secrete antimicrobial peptides and mucin glycoproteins, form an antimicrobial barrier that is critical for the maintenance of intestinal homeostasis (Bevins and Salzman, 2011).

Disturbance of endoplasmic reticulum (ER) homeostasis has been implicated in the pathogenesis of IBD (Heazlewood *et al.*, 2008; Kaser *et al.*, 2008, 2013; Adolph *et al.*, 2013; Das *et al.*, 2013). ER-associated degradation (ERAD) is a principal quality-control mechanism in the cell, targeting misfolded proteins for cytosolic degradation (Olzmann *et al.*, 2013). Whereas the biochemical

This article was published online ahead of print in MBoC in Press (http://www.molbiolcell.org/cgi/doi/10.1091/mbc.E15-10-0724) on December 2, 2015.

*Present address: Department of Pharmacology, University of Texas Southwestern Medical Center, Dallas, TX 75390.

S.S. and L.Q. designed the research; S.S., R.L., S.B.C., Y.J., J.K.G., A.C.P., G.E.D., and K.W.S. performed most of the experiments; Q.L. contributed the Sel1L floxed mice; S.S., R.L., S.B.C., Y.J., J.K.G., A.C.P., R.E.L., E.Y.D., M.A.M., G.E.D., K.W.S., and L.Q. analyzed data; S.S. and L.Q. wrote the manuscript; and all authors edited and approved the manuscript.

Address correspondence to: Shengyi Sun (ss2475@cornell.edu), Ling Qi (lq35@cornell.edu).

Abbreviations used: CD, Crohn's disease; DSS, dextran sodium sulfate; ER, endoplasmic reticulum; ERAD, ER-associated degradation; FISH, fluorescence in situ hybridization; IBD, inflammatory bowel disease; IEC, intestinal epithelial cell; IgG, immunoglobulin G; PBS, phosphate-buffered saline; RT-qPCR, reverse-transcription quantitative PCR; TEM, transmission electron microscopy; UC, ulcerative colitis; UPR, unfolded protein response.

© 2016 Sun *et al.* This article is distributed by The American Society for Cell Biology under license from the author(s). Two months after publication it is available to the public under an Attribution–Noncommercial–Share Alike 3.0 Unported Creative Commons License (http://creativecommons.org/licenses/by-nc-sa/3.0).

"ASCB®," "The American Society for Cell Biology®," and "Molecular Biology of the Cell®" are registered trademarks of The American Society for Cell Biology.

processes of ERAD have been well characterized, the physiological significance of ERAD and its role in the pathogenesis of IBD are undefined. The E3 ligase Hrd1 and its cofactor Sel1L (Hrd3p in yeast) represent the most highly conserved branch of the mammalian ERAD (Travers *et al.*, 2000; Yoshida *et al.*, 2003; Kaneko *et al.*, 2007; Christianson *et al.*, 2012). The Sel1L-Hrd1 complex is responsible for the recognition and retrotranslation of a subset of misfolded proteins in the ER directed for cytosolic proteasomal degradation (Olzmann *et al.*, 2013; Christianson and Ye, 2014). The specific function of Sel1L-Hrd1 ERAD has been difficult to assess due to the embryonic lethality of Sel1L- or Hrd1-deficient mice (Yagishita *et al.*, 2005; Francisco *et al.*, 2010). Defining the role of the ERAD machinery in specific cell types could lead to the identification of molecular pathways underpinning ERAD-associated physiology and disease.

Conditional knockout mouse and cell models deficient in Sel1L provide in vivo evidence that Sel1L is an indispensable component of mammalian E3 ligase Hrd1 ERAD complex (Sun *et al.*, 2014). In adipocytes, Sel1L is required for diet-induced obesity and the development of postprandial hypertriglyceridemia by regulating the ER exit of lipoprotein lipase (Sha *et al.*, 2014). In a recent study, we identified IRE1α, the sensor of unfolded protein response (UPR), as an endogenous Sel1L-Hrd1 ERAD substrate (Sun *et al.*, 2015). Sel1L-Hrd1 ERAD degrades IRE1α under basal conditions in a BiP-dependent manner. ER stress triggers the dissociation of IRE1α from the ERAD complex, leading to IRE1α accumulation and activation.

To dissect the physiological significance of Sel1L and Sel1L-Hrd1 ERAD-mediated IRE1α degradation, we generated intestinal epithelial cell–specific Sel1L-deficient (*Sel1L*$^{\Delta IEC}$) mice (Sun *et al.*, 2015). Surprisingly, epithelial Sel1L is dispensable for the overall morphology of the colon under basal conditions; however, Sel1L deficiency increases sensitivity to DSS-induced experimental colitis. This is in part mediated through stabilization and accumulation of IRE1α protein in colonic epithelium (Sun *et al.*, 2015). How Sel1L and Sel1L-Hrd1 ERAD affect the function of the small intestine remains to be demonstrated. Here we show that expression of epithelial SEL1L and HRD1 is inversely correlated with the severity of ileal inflammation in individuals with CD. Further mechanistic studies in mice provide definitive evidence for a critical role of epithelial Sel1L-Hrd1 ERAD in spontaneous enteritis and hypersensitivity to pathogens.

## RESULTS

### Expression of SEL1L and HRD1 in CD

To explore a possible role of SEL1L-HRD1 ERAD in CD, we determined the gene expression pattern of *SEL1L* and *HRD1* in ileal tissues from CD patients. Intriguingly, expression of *SEL1L* was tightly correlated with that of *HRD1* (Figure 1A) and was reduced by nearly 10-fold with inflammation (Figure 1B, Supplemental Figure S1A, and Supplemental Table S1). Similar observations were made for *HRD1*, albeit to a lesser extent (Figure 1B and Supplemental Figure S1A). Expression of *SEL1L* and *HRD1* was also positively correlated with the expression of UPR effectors and ER chaperones, such as *XBP1s*, *HSP5A*, and *CALRETICULIN* (Supplemental Figure S1, B and C). These results demonstrate down-regulation of SEL1L-HRD1 in the inflamed small intestine of human patients with IBD, pointing to a possible role of ERAD in disease pathogenesis.

### An epithelia-specific mouse model defective in Sel1L-Hrd1 ERAD

To test directly the pathophysiological role of Sel1L-Hrd1 ERAD in intestinal inflammation, we generated intestinal epithelial cell (IEC)–specific, Sel1L-deficient mice (*Sel1L*$^{\Delta IEC}$) by crossing *Sel1L*$^{flox/flox}$ mice

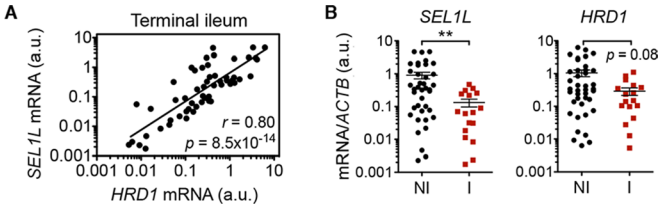


FIGURE 1: Human studies link SEL1L-HRD1 ERAD to intestinal inflammation. (A) Correlations between *SEL1L* and *HRD1* expression in human terminal Ileum. (B) qPCR analysis of *SEL1L* and *HRD1* expression in terminal Ileum samples from patients with or without inflammation. Inflammatory score is based on criteria in Supplemental Table S1. NI, noninflammation (score ≤ 2); I, inflammation (score ≥ 3). Values, mean ± SEM. $^{**}p < 0.01$ by Mann–Whitney test. Spearman's *r* value was calculated for correlations.

(Sun *et al.*, 2014) with Villin-Cre transgenic mice. Reduction of Sel1L and Hrd1 protein was observed in the small intestine of *Sel1L*$^{\Delta IEC}$ mice (Figure 2, A–C). Indeed, these mice were defective in ERAD function, as demonstrated by the accumulation of the known substrate OS9 in IEC (Sha *et al.*, 2014; Sun *et al.*, 2014; Figure 2, A and B). Thus *Sel1L*$^{\Delta IEC}$ mice are defective in Sel1L-Hrd1 ERAD function in the small intestine.

### Epithelial Sel1L deficiency leads to spontaneous enteritis

Of interest, the small intestine villi of *Sel1L*$^{\Delta IEC}$ mice were blunted, and the lamina propria at the tip of the villi contained large clusters of plasma cells and many eosinophils (Figure 3, A and B), similar to those seen in lymphoplasmacytic (Ochoa *et al.*, 1984) and eosinophilic enteritis (Baig *et al.*, 2006) in humans (Odze, 2003). Immunofluorescence staining identified immunoglobulin G (IgG)-positive B-cells at the tip of intestinal villi of *Sel1L*$^{\Delta IEC}$ mice, whereas in wild-type (WT) mice, these cells were present at the base of the villi (Figure 3C). In line with elevated inflammation, the intestinal crypts in the duodenum of *Sel1L*$^{\Delta IEC}$ mice were longer and contained an expanded population of epithelial cells expressing Ki67 and

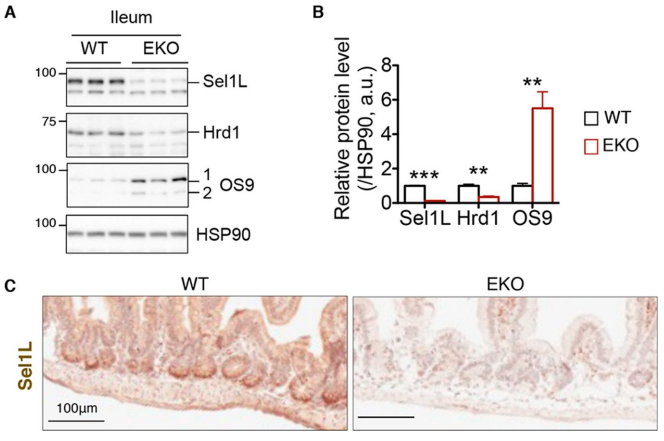


FIGURE 2: Generation of epithelial-specific Sel1L-deficient mice. (A, B) Western blot analysis of Sel1L-Hrd1 ERAD protein levels in the terminal ileum of WT and *Sel1L*$^{\Delta IEC}$ mice. (B) Quantitation. Each lane represents an independent sample. HSP90, loading control. (C) Immunohistochemistry staining of Sel1L in ileum of WT and *Sel1L*$^{\Delta IEC}$ (EKO) mice, showing Sel1L depletion in epithelium. All experiments were repeated at least twice, with three mice each. Values, mean ± SEM. $^{**}p < 0.01$ and $^{***}p < 0.001$ by Student's *t* test.

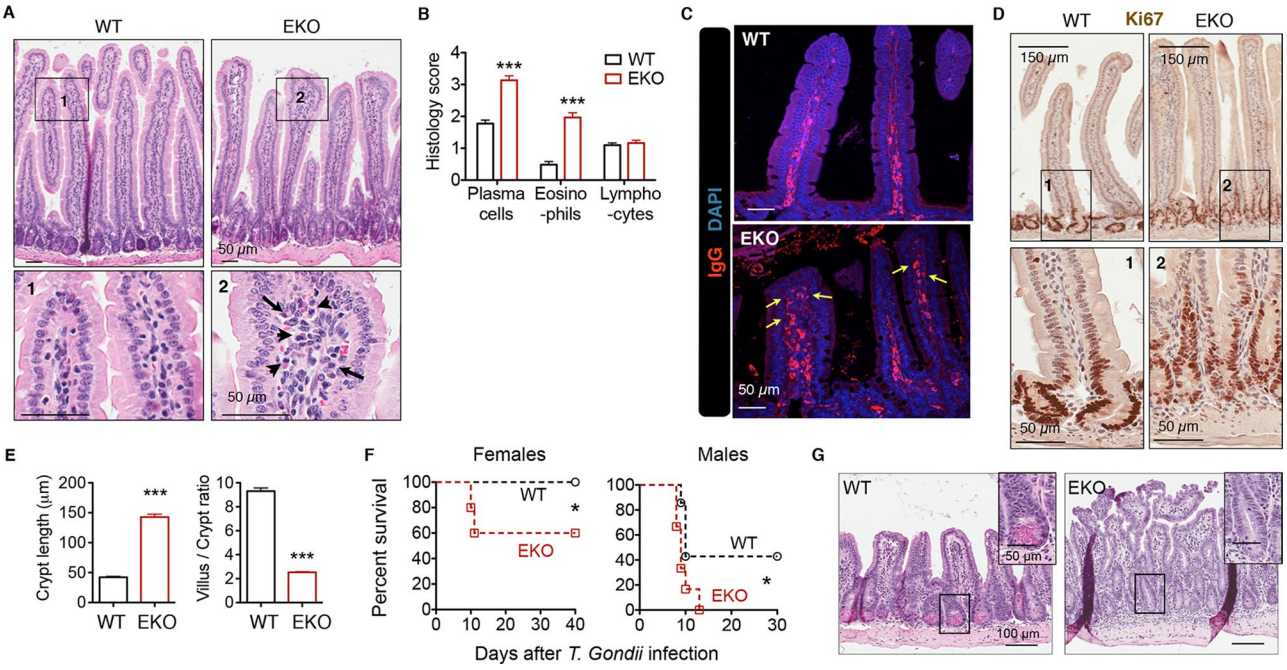


FIGURE 3: *Sel1L*$^{\Delta IEC}$ (EKO) mice are predisposed to spontaneous enteritis and *T. gondii* infection. (A) Representative hematoxylin and eosin (H&E) images of duodenum and villus tips in 14-wk-old WT and EKO mice, showing partial villous blunting, plasmacytosis (arrowheads), and eosinophilic enteritis (arrows)—signs of spontaneous enteritis. (B) Histology score of the presence and distribution of lymphocytes, plasma cells, and eosinophils within the lamina propria of intestinal villi and crypts of duodenum as a blind study. Thirty 400 × fields. Scoring: 0, none; 1, rare; 2, few scattered; 3, many groups; 4, large numbers. (C) Immunofluorescence staining of plasma cells (red) in duodenum, showing clusters of IgG-positive plasma cells at the tip of the villi (arrows) of *Sel1L*$^{\Delta IEC}$ mice. (D) Immunohistochemistry staining of Ki67 in duodenum, showing mild crypt hyperplasia in EKO mice. (E) Quantitation of crypt length and villus-to-crypt ratio in duodenum as measured from 30 villus-crypt units. All experiments were repeated at least twice with three mice each. Values, mean ± SEM. ***$p < 0.001$ by Student's *t* test. (F) Survival curves of female and male *Sel1L*$^{\Delta IEC}$ mice after *T. gondii* infection. *$p < 0.05$ by the log-rank Mantel–Cox test. Five mice each. (G) Representative H&E images of ileum 7 d after *T. Gondii* infection, with inset showing the boxed area.

reduced villus-to-crypt ratio relative to WT mice (Figure 3, D and E). Thus epithelial Sel1L deficiency in the small intestine leads to spontaneous lymphoplasmacytic and eosinophilic enteritis.

## Epithelial Sel1L is required for resistance to pathogen infection

To determine whether Sel1L-Hrd1 ERAD deficiency influences intestinal response to pathogen infection, we infected mice with *Toxoplasma gondii*, which causes a granulomatous Th1-dominated ileitis and proliferation of *Escherichia coli* that recapitulates many of the features of CD ileitis (Egan *et al.*, 2012). Both male and female *Sel1L*$^{\Delta IEC}$ mice exhibited increased disease susceptibility and lethality to *T. gondii* infection (Figure 3F). Histological analyses revealed more severe ileitis in *Sel1L*$^{\Delta IEC}$ mice, with generalized villous stunting, Paneth cell loss, and crypt hyperplasia associated with massive inflammatory cell infiltration (Figure 3G). Fluorescence in situ hybridization (FISH) analysis revealed increased adherence and invasion of eubacteria and *E. coli* in the ileal mucosa of *Sel1L*$^{\Delta IEC}$ mice compared with WT littermates (Supplemental Figure S2, A and B). Thus epithelial Sel1L-Hrd1 ERAD is required for protection against pathogen infection in the small intestine.

## Epithelial Sel1L is required for Paneth cell function

In the small intestine, Sel1L was ubiquitously expressed in the epithelium and highly enriched in lysozyme C–positive Paneth cells at the base of crypts (Figure 4, A and B). Paneth cells comprise a specialized cell population in the small intestine that secretes antimicrobial peptides from secretory granules. Sel1L deficiency dramatically reduced eosinophilic secretory granules in Paneth cells (Figure 5A), resembling variable Paneth cell abnormalities in human CD patients involving the terminal ileum (Liu *et al.*, 2014; VanDussen *et al.*, 2014). Protein levels of the antimicrobial peptides lysozyme C and RegIIIγ were greatly reduced (Figure 5, B–D). Indeed, expression of a panel of antibacterial peptides, including *lysozyme* and *RegIIIγ*, was reduced in the small intestine of *Sel1L*$^{\Delta IEC}$ mice (Figure 5E). Transmission electron microscopy (TEM) of the ileum revealed dilated and fragmented ER cisternae, as well as "fried egg"–shaped secretory vesicles with centrally located granules in Paneth cells of *Sel1L*$^{\Delta IEC}$ mice (Figure 5F). Thus Sel1L-Hrd1 ERAD is required for the secretory function of Paneth cells.

## Epithelial Sel1L deficiency alters gut microbiota composition

Studies have shown that the secretory function of Paneth cells influences intestinal bacterial overgrowth and gut microbiota composition (Ayabe *et al.*, 2000; Vaishnava *et al.*, 2008). To delineate how epithelial Sel1L deficiency affects gut microbiota composition, we performed microbiota sequencing of fecal samples from *Sel1L*$^{\Delta IEC}$ and cohoused WT littermates using culture-independent PCR amplification of variable region 4 (V4) of bacterial 16S rRNA genes (Ji *et al.*, 2014). The multiplexed amplicons were subjected to Illumina

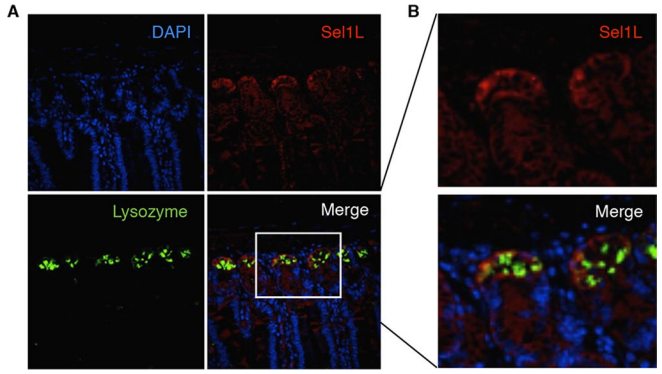


FIGURE 4: Sel1L is highly enriched in Paneth cells. (A, B) Confocal images of Sel1L (red) and lysozyme C (green) in small intestines of WT mice showing enrichment of Sel1L in Paneth cells at the base of the crypts. A close-up view of the boxed area is shown in B.

sequencing using the Mi-Seq platform. The overall microbial profiles were expectedly similar between cohoused WT littermates and *Sel1L*$^{\Delta IEC}$ mice as shown previously (Sun *et al.*, 2015). However, in-depth analysis revealed a 10-fold increase of *Ruminococcus gnavus*, a Gram-positive anaerobic bacterium (Dethlefsen *et al.*, 2006), in *Sel1L*$^{\Delta IEC}$ mice compared with cohoused WT littermates (Figure 5, G and H). Because *R. gnavus* is not overrepresented in other mouse strains bred in our colony (Ji *et al.*, 2014), this expansion appears to be directly linked to the absence of epithelial Sel1L. Thus epithelial Sel1L deficiency influences microbiota composition.

### Epithelial Sel1L deficiency induces ER stress and cell death in small intestine

In keeping with our previous report that IRE1α is an ERAD substrate (Sun *et al.*, 2015), IRE1α protein level elevated by >20-fold in the small intestine of *Sel1L*$^{\Delta IEC}$ mice, whereas its mRNA level was not affected (Figure 6, A, B, and D). IRE1α was moderately activated, as measured by mobility shift of IRE1α protein in a Phos-tag gel (Sha *et al.*, 2009; Yang *et al.*, 2010; Qi *et al.*, 2011) and its substrate *Xbp1* mRNA splicing (Figure 6, A and E). IRE1α activation was in line with the activation of other UPR markers, including PERK and eIF2α phosphorylation, as well as elevated expression of various downstream effectors and ER chaperones (Figure 6, A–D). Furthermore, epithelial cell death in the small intestine was increased in *Sel1L*$^{\Delta IEC}$ mice under

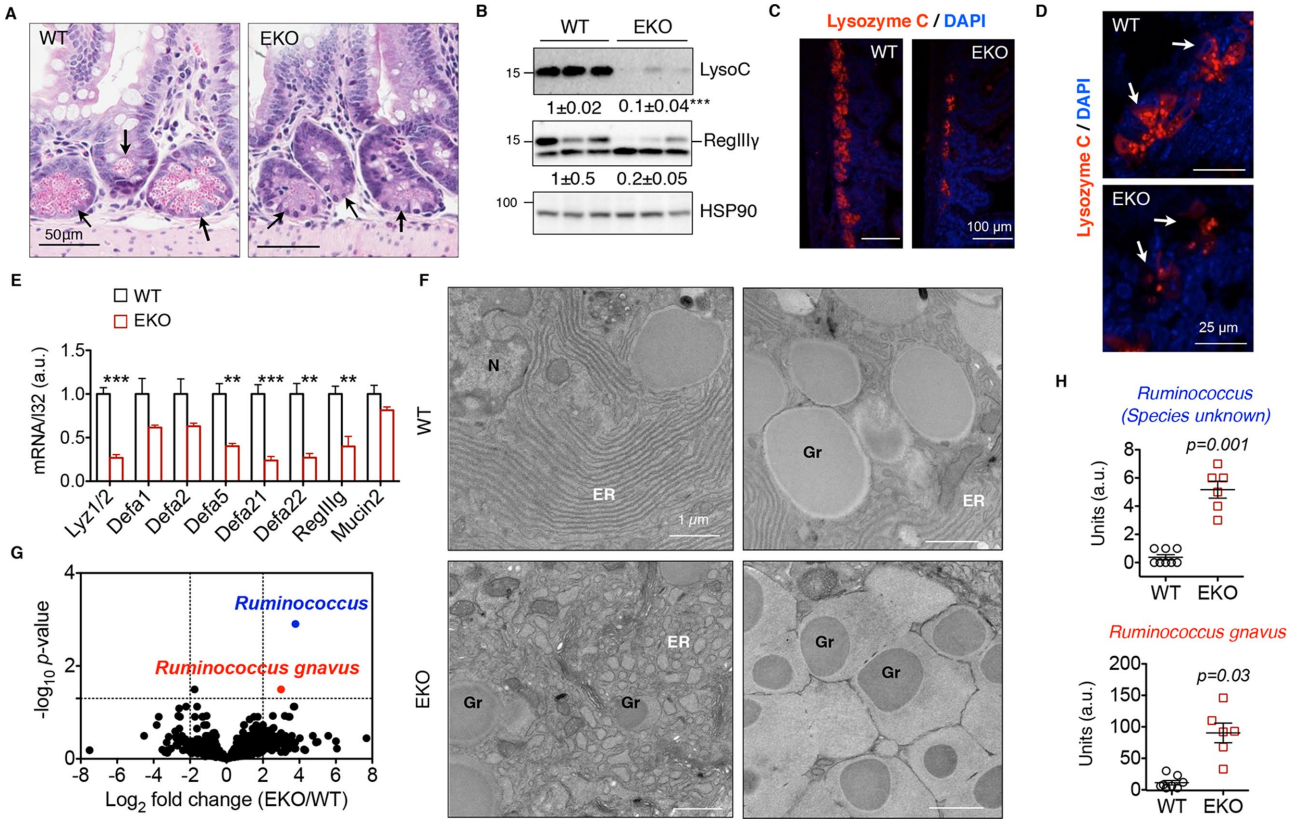


FIGURE 5: Sel1L is required for Paneth cell function and the expression of antimicrobial peptides. (A) Representative H&E images of ileal crypts of 14-wk-old *Sel1L*$^{\Delta IEC}$ mice showing shrunken eosinophilic granules in the Paneth cells (arrow) of *Sel1L*$^{\Delta IEC}$ mice. (B) Western blot analysis of lysozyme C and RegIIIγ in the terminal ileum, with quantitation shown below the blots. (C, D) Confocal microscopic images of lysozyme C labeling of Paneth cells at the crypts of the terminal ileum at low (C) and high (D) magnifications. (E) qPCR analysis of antibacterial peptide expression in ileum of WT and *Sel1L*$^{\Delta IEC}$ mice. Experiments were repeated twice with three mice each. Values, mean ± SEM. $^{**}p < 0.01$ and $^{***}p < 0.001$ by Student's *t* test. (F) Representative TEM images of Paneth cells at the terminal ileum. Note the reduced size of secretory granules (Gr) and fried egg–shaped secretory vesicles in Paneth cells of *Sel1L*$^{\Delta IEC}$ mice. ER, endoplasmic reticulum; N, nucleus. (G, H) Volcano plots showing significantly different abundance of bacterial operational taxonomic units (OTUs) on comparing *Sel1L*$^{\Delta IEC}$ to cohoused WT littermates. The two vertical reference lines indicate a fourfold change (log2), and the horizontal line represents $p < 0.05$ (–log10) by Student's *t* test followed by Benjamini–Hochberg correction. Two OTUs significantly enriched in *Sel1L*$^{\Delta IEC}$ mice are shown in H. For microbiota analysis, WT, $n = 7$; EKO, $n = 6$. Values, mean ± SEM. a.u., arbitrary units. The *p* values by Student's *t* test followed by Benjamini–Hochberg correction.

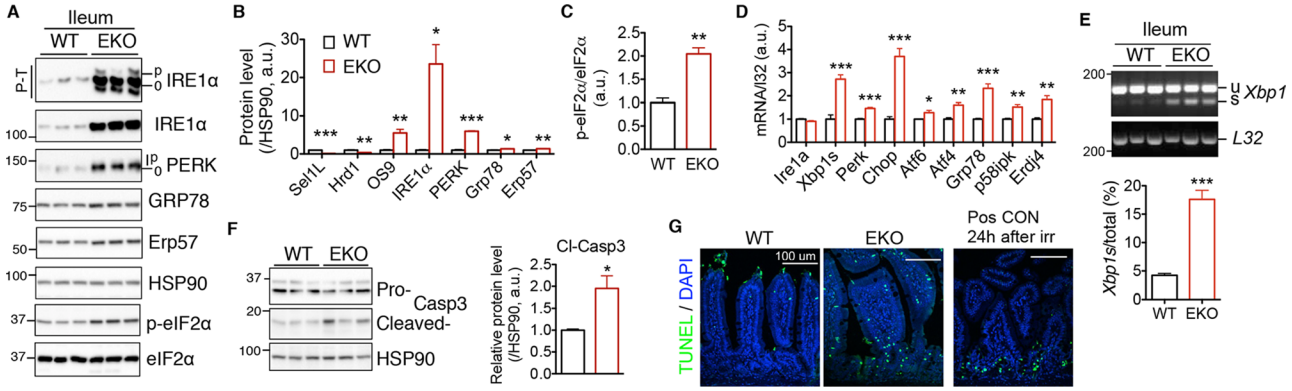


FIGURE 6: Sel1L is required for the ER homeostasis in the epithelium of small intestines. (A–C) Western blot analysis of IRE1α, PERK, ER chaperones, and phosphorylated eIF2α in the ileum. Each lane represents an independent sample, and quantitation is shown in B. P-T, Phos-tag–based Western blot analysis of IRE1α phosphorylation. HSP90, loading control. (C) Quantitation of eIF2α phosphorylation in ileum. (D) qPCR analysis of mRNA levels in the ileum. (E) RT-PCR analysis of *Xbp1* mRNA splicing, with quantitation shown below. (F) Western blot analysis of caspase-3 cleavage in the ileum, with quantitation shown on the right. (G) Confocal images of terminal deoxynucleotidyl transferase dUTP nick-end labeling (TUNEL) staining of terminal ileum, showing elevated cell death in the crypts of *Sel1L*$^{\Delta IEC}$ mice. The ileum from WT mice 24 h after 10 Gy irradiation (irr) was used as positive control (Pos CON). All experiments were repeated at least twice with three mice each. Values, mean ± SEM. *$p < 0.05$, **$p < 0.01$, and ***$p < 0.001$ by Student's *t* test.

basal conditions, as demonstrated by caspase 3 cleavage (Figure 6F). Histological analyses revealed clustered cell death in both villi and the crypts of small intestine of *Sel1L*$^{\Delta IEC}$ mice but only at the tips of the villi in WT mice (Figure 6G). Thus epithelial Sel1L regulates ER homeostasis and cell survival in the small intestine.

### Lack of epithelial Sel1L haploinsufficiency

To address whether Sel1L heterozygosity affects intestinal homeostasis, we generated and characterized *Sel1L*$^{\Delta IEC/+}$ (HET) mice. Unlike *Sel1L*$^{\Delta IEC}$ littermates, *Sel1L*$^{\Delta IEC/+}$ mice did not develop enteritis (Supplemental Figure S3A) or Paneth cell atrophy in the small intestine (Supplemental Figure S3, B–E). ER homeostasis in the epithelium of small intestines was not affected by Sel1L heterozygosity (Supplemental Figure S3B). This result suggests that one copy of Sel1L is sufficient to maintain Paneth cell function and homeostasis in the small intestine.

### IRE1α is dispensable for intestinal pathologies of *Sel1L*$^{\Delta IEC}$ mice

UPR sensor IRE1α may link ER stress to inflammation and cell death (Hetz, 2012). IRE1α accumulated and was mildly activated in the small intestine of *Sel1L*$^{\Delta IEC}$ mice (Figure 6). To determine whether IRE1α activation is responsible, at least in part, for the intestinal abnormalities in *Sel1L*$^{\Delta IEC}$ mice, we generated and characterized epithelium-specific *Sel1L*$^{\Delta IEC}$;*Ire1a*$^{\Delta IEC}$ mice (Figure 7, A and B). Both IRE1α protein and *Xbp1s* mRNA were abolished in the double-knockout mice (Figure 7, A and B). Surprisingly, loss of IRE1α failed to alter ERAD deficiency–induced enteritis (Figure 7C), Paneth cell atrophy (Figure 7, D–F), or cell death (Figure 7, G and H) in the small intestines of *Sel1L*$^{\Delta IEC}$ mice. Thus Sel1L deficiency–associated abnormalities of the small intestines are not mediated by IRE1α.

### C/EBP homologous protein is dispensable for intestinal pathologies of *Sel1L*$^{\Delta IEC}$ mice

C/EBP homologous protein (CHOP), a downstream effector of the PERK pathway of the UPR, may link ER stress to cell death (Hetz, 2012). *Chop* mRNA was upregulated by fourfold in the small intestine of *Sel1L*$^{\Delta IEC}$ mice (Figure 6D). To determine whether *Chop* is responsible, at least in part, for the intestinal pathologies of *Sel1L*$^{\Delta IEC}$ mice, we generated and characterized *Sel1L*$^{\Delta IEC}$ mice on the *Chop*$^{-/-}$ background. Of interest, CHOP was not responsible for ERAD deficiency–induced enteritis (Supplemental Figure S4A), Paneth cell atrophy (Supplemental Figure S4, B and C), or cell death (Supplemental Figure S4, D and E). In aggregate, we conclude that Sel1L deficiency–associated abnormalities of the small intestine are not mediated by IRE1α and CHOP.

## DISCUSSION

The physiological importance of ERAD complexes in vivo is largely unknown. We generated the first enterocyte-specific, Sel1L-Hrd1 ERAD–deficient mouse model, allowing the investigation of a new pathway in the pathogenesis of IBD. Of interest, *Sel1L*$^{\Delta IEC}$ mice develop spontaneous inflammation in the small intestine (as discussed here) but have few abnormalities in the colon (Sun *et al.*, 2015). Differences in the regional distribution of inflammation between colon and ileum are frequently observed in human IBD, with CD frequently restricted to the small intestine and UC restricted to the colon. The decreased SEL1L and HRD1 expression in the ileal mucosa of patients with CD suggests a potentially causal effect of SEL1L-HRD1 ERAD in disease pathogenesis. Moreover, epithelial Sel1L deficiency is associated with the enrichment of *R. gnavus* in the fecal pellets. Previous studies sowed that *R. gnavus* is mucolytic (i.e., degrades mucin; Hoskins and Boulding, 1981; Hoskins *et al.*, 1985) and is particularly overrepresented in human patients (Prindiville *et al.*, 2004; Png *et al.*, 2010; Willing *et al.*, 2010; Joossens *et al.*, 2011). Whether *R. gnavus* is responsible for the pathology of *Sel1L*$^{\Delta IEC}$ mice remains to be established using monoassociation studies.

Different cell types have distinct requirements for protein folding and disposal and hence for Sel1L-Hrd1 ERAD. Comparative analysis of the cellular response to ERAD deficiency in different cell types may provide important insights into tissue- or organ-specific functions of ERAD. Paneth and pancreatic acinar cells have a strict requirement of Sel1L-Hrd1 ERAD (Sun *et al.*, 2014; present results), whereas Sel1L-Hrd1 ERAD seems dispensable for the normal physiology of adipocytes and intestinal goblet cells (Sha *et al.*, 2014; Sun *et al.*, 2014, 2015). The differential requirement of ERAD is likely due to the diversity and amount of the proteins synthesized in specific

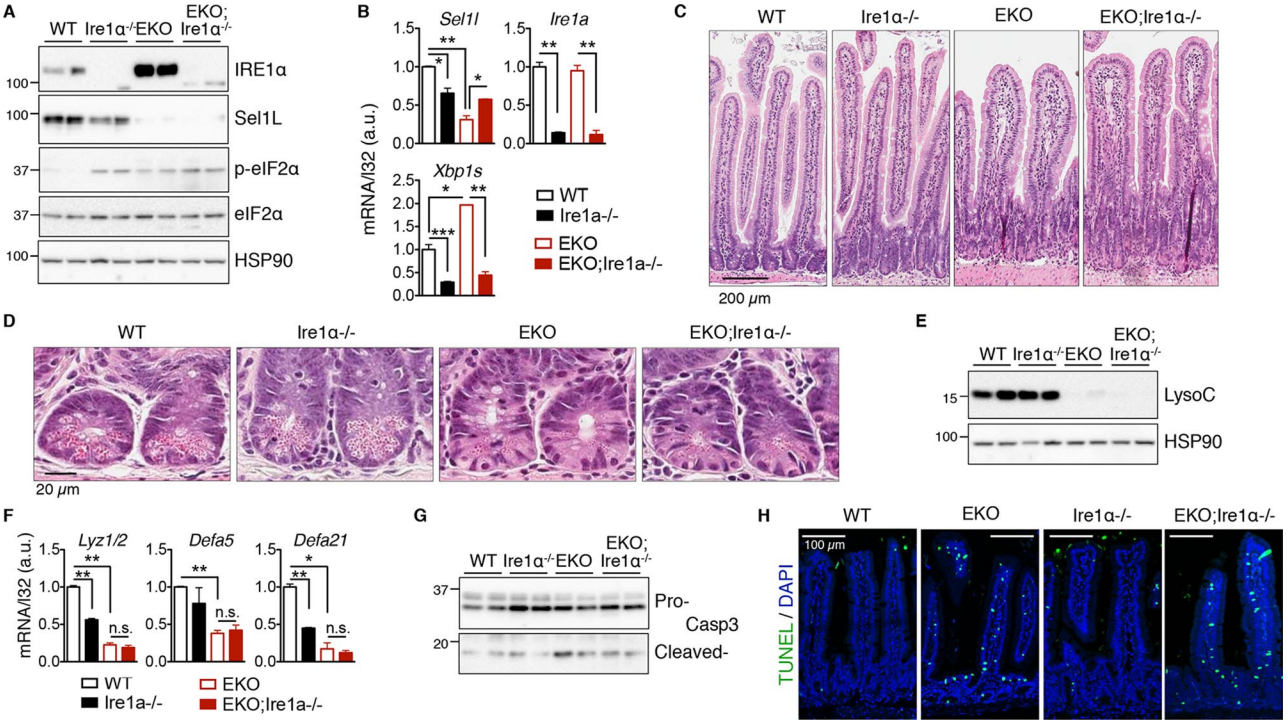


FIGURE 7: The effect of epithelial Sel1L in the small intestines is independent of IRE1α. (A, B) Western blot and qPCR analyses in terminal ileum of WT, *Ire1af/f;VillinCre*$^{+}$ (enterocyte-specific *Ire1a*$^{-/-}$), EKO, and EKO;*Ire1a*$^{-/-}$ littermates, showing levels of Sel1L, IRE1α, and various UPR markers. (C, D) Representative H&E images of duodenum (C) and ileum (D), showing spontaneous enteritis and Paneth cell defect, respectively. (E, F) Western blot and qPCR analyses in terminal ileum showing the expression of antibacterial peptides. (G, H) Western blot and TUNEL analyses of terminal ileum. All experiments were repeated at least twice with three or four mice. Values, mean ± SEM. *$p < 0.05$, ** $p < 0.01$, and ***$p < 0.001$ by Student's *t* test.

cells. Cell type–specific ERAD function and endogenous ERAD substrates are open areas for further investigation.

Disturbance of ER homeostasis has been implicated in the pathogenesis of human CD and UC (Heazlewood *et al.*, 2008; Kaser *et al.*, 2008, 2013; Adolph *et al.*, 2013; Das *et al.*, 2013). In addition to ERAD, ER homeostasis is monitored by another highly conserved protein quality-control system known as UPR. In the last several years, the role of UPR in gut epithelium in the context of IBD has been increasingly appreciated, with the characterization of enterocyte-specific UPR-deficient mice such as *XBP1*$^{\Delta IEC}$, *IRE1α*$^{\Delta IEC}$, and *CHOP*$^{-/-}$ mice (Bertolotti *et al.*, 2001; Kaser *et al.*, 2008, 2013; Namba *et al.*, 2009; Park *et al.*, 2009; Zhao *et al.*, 2010; Adolph *et al.*, 2013; Niederreiter *et al.*, 2013; Tsuru *et al.*, 2013). *Xbp1* mRNA is spliced by IRE1α in response to ER stress, leading to the generation of a stabilized transcription factor XBP1s to regulate ER homeostasis. In *Xbp1*-deficient intestinal epithelium, IRE1α is hyperactivated, which promotes the development of spontaneous intestinal inflammation via the activation of inflammatory mediators such as JNK (Kaser *et al.*, 2008; Adolph *et al.*, 2013). In contrast, the loss of epithelial IRE1α does not affect Paneth cell function or cause spontaneous colitis in mice at a young age (Zhang *et al.*, 2015; this study), suggesting the importance of the unspliced form of XBP1 in the maintenance of gut homeostasis. CHOP is a transcription factor induced under ER stress and is believed to mediate ER stress–induced apoptosis. *CHOP*$^{-/-}$ mice were protected from dextran sodium sulfate (DSS)–induced colitis (Namba *et al.*, 2009). In our studies, Sel1L-Hrd1 ERAD deficiency causes dramatic accumulation and activation of both IRE1α and CHOP in the epithelia of both small (this study) and large intestines (Sun *et al.*, 2014). In the colon, IRE1α heterozygosity partially rescues the DSS sensitivity of the *Sel1L*$^{\Delta IEC}$ mice, whereas CHOP was dispensable (Sun *et al.*, 2015). By contrast, in the present study, neither IRE1α nor CHOP was involved in the pathogenesis of the small intestinal abnormalities observed in *Sel1L*$^{\Delta IEC}$ mice. Moreover, *Sel1L*$^{\Delta IEC}$ mice exhibit unique phenotypes, including spontaneous plasmacytic and eosinophilic enteritis and a disproportionate increase of mucolytic and potentially pathogenic *R. gnavus* compared with previous UPR models (Bertolotti *et al.*, 2001; Kaser *et al.*, 2008; Park *et al.*, 2009; Zhao *et al.*, 2010; Adolph *et al.*, 2013; Niederreiter *et al.*, 2013; Tsuru *et al.*, 2013). Thus the physiological effect of Sel1L-Hrd1 ERAD in the small intestine is likely to be mediated by other UPR branches or UPR-independent mechanisms. Future investigations are warranted to identify other endogenous ERAD substrates or associated signaling pathways to elucidate their importance in the pathogenesis of IBD.

In addition to ERAD and UPR, autophagy has been implicated as an important regulator of Paneth cell biology and protein homeostasis in the ER (Cadwell *et al.*, 2008; Adolph *et al.*, 2013). The interplay among ERAD, UPR, and autophagy, however, has not been tested in vivo. The generation and characterization of compound mouse models will be critical to delineate how they function cooperatively in a cell type–specific manner in vivo.

## MATERIALS AND METHODS

### Mice

Cell type–specific *Sel1L*$^{\Delta IEC}$, *Sel1L*$^{\Delta IEC/+}$, *Sel1L*$^{\Delta IEC}$;*Chop*$^{-/-}$, and *Sel1L*$^{\Delta IEC}$;*Ire1a*$^{-/-}$ mice were used in this study. *Sel1L*$^{flox/flox}$ mice on the C57BL/6J background have been described (Sun *et al.*, 2014,

2015) and were crossed with villin 1 promoter–driven Cre mice (B6. SJL-Tg(Vil-Cre)997Gum/J, JAX 004586, Bar Harbor, ME), which have been backcrossed to the C57BL/6J background for more than five generations. Mice were housed under specific pathogen-free conditions and fed on a low-fat diet consisting of 13% fat, 67% carbohydrate, and 20% protein (Harlan Teklad 2914, Madison, WI). Cohoused age-matched adult littermates were used at the age of 8–12 wk in all in vivo experiments. Killing of animals was performed by cervical dislocation. Intestinal tissues were immediately harvested and either fixed in 10% neutralized Formalin for histology or flushed with phosphate-buffered saline (PBS) and snap-frozen in liquid nitrogen for protein and RNA analyses. Frozen tissues were stored at –80°C. All animal procedures were approved by the Institutional Animal Care and Use Committee at Cornell University.

### Histological analysis

Tissues were fixed in 10% neutralized Formalin and processed by the Cornell Histology Core Facility as described (Sun *et al.*, 2015). Sections of proximal small intestine were scored for the presence and distribution of lymphocytes, plasma cells, and eosinophils within the lamina propria of intestinal villi and crypts in thirty 400× fields (0, none; 1, rare; 2, few scattered; 3, many groups; 4, large numbers) blinded to treatment group (Garner *et al.*, 2009). Crypt and villus length in the proximal small intestine was measured for 30 villous:crypt (V:C) units.

### *T. gondii* infection

Pathogen infection was performed as previously described (Cohen and Denkers, 2015). Briefly, *T. gondii* cysts of the type II ME49 strain were passaged in vivo through sublethal infection of female Swiss Webster mice (6–8 wk of age, JAX). Cysts were harvested from chronically infected Swiss Webster mice by whole-brain homogenization in sterile PBS. For infection of *Sel1L*$^{\Delta IEC}$ mice, 30 cysts of *T. gondii* were administered by oral gavage in 200 µl of PBS and monitored daily. Mice were killed on day 7, and intestines were fixed in Formalin for histology. For survival curve, mice were followed until the time indicated in the graph and killed.

### FISH

Formalin-fixed, paraffin-embedded intestine sections were mounted on Probe-On Plus slides (Fisher, Pittsburgh, PA) and evaluated by FISH with probes to all bacteria (EUB338-5′Cy3) or *E. coli/Shigella* (*E. coli*-5′Cy3, 16SrRNA), in combination with a nonspecific binding control probe (non-EUB338-5′FAM; IDT, Coralville, IA), as previously described (Simpson *et al.*, 2006; Baumgart *et al.*, 2007). Sections were examined with an Olympus BX51 epifluorescence microscope, and images were captured with an Olympus DP-7 camera.

### Microbiota sequencing and analysis

Fecal samples were collected from 8-wk-old mice and analyzed as previously described (Ji *et al.*, 2014). To identify bacteria that were significantly altered, *p* values were calculated by unpaired two-tailed Student's *t*-test and corrected by the Benjamini–Hochberg procedure. $p < 0.05$ was considered statistically significant.

### Human IBD samples, RNA extraction, and quantitative PCR analysis

Terminal ileum tissue biopsies ($n = 57$) were obtained at endoscopy from 11 UC patients (7 noninflamed and 4 inflamed mucosa), 20 CD patients (11 noninflamed and 9 inflamed mucosa), and 7 miscellaneous and 19 healthy individuals (control group) as previously described (Sheng *et al.*, 2011). Inflammation was scored by an in-house scheme as shown in Supplemental Table S1. Biopsies were considered "inflamed" with inflammation scores ≥3. All patients gave informed consent for the procedure. The study was approved by the Mater Health Services Health and Research Ethics Committee. Total RNA was extracted by RNeasy Plus Mini Kit (Qiagen, Valencia, CA), and all RNA samples had RNA integrity number or RNA quality indicator value of >3. Reverse-transcription (RT) quantitative PCR (qPCR) analysis was performed with Bio-Rad Viia 7 (Life Technologies, Carlsbad, CA) using a SensiFASTTM SYBR Lo-Rox kit (Bioline, Meridian Life). Primer sequences are listed in Supplemental Table S2. The qPCR data for human tissues were normalized to β-actin (*ACTB*) in the corresponding sample. Fold changes were calculated by the ΔΔ method and normalized to the control group.

### Statistical analysis

Results are expressed as mean ± SEM. Comparisons between groups were made by unpaired two-tailed Student's *t*-test unless otherwise indicated. Survival curves were compared by the log-rank (Mantel–Cox) test. $p < 0.05$ was considered statistically significant. All experiments were repeated at least two to three times, and representative data are shown. For human studies, the Mann–Whitney test was used for comparisons to generate *p* values, and Spearman's *r* values were calculated for correlations.

## ACKNOWLEDGMENTS

We thank Lora Hooper (UT Southwestern, Dallas, TX) for generous gifts of antibodies and other members of the Qi lab for comments, suggestions, and technical assistance. This work was supported by National Institutes of Health Grants R21AI085332 (G.D.) and R21AI09061 (E.Y.K.), Chinese National Natural Science Foundation Grant 31371391 (to Q.L.), National Institutes of Health Grants 1R01GM113188 and 1R01DK105393, Juvenile Diabetes Research Foundation Grant 47-2012-767, and American Diabetes Association Grant 1-12-CD-04 (L.Q.). S.S. is an International Student Research Fellow of the Howard Hughes Medical Institute (59107338). R.L. is the recipient of a Betty McGrath Mater Practitioner Research Fellowship. L.Q. is the recipient of Junior Faculty and Career Development Awards from the American Diabetes Association.

## REFERENCES

Adolph TE, Tomczak MF, Niederreiter L, Ko HJ, Bock J, Martinez-Naves E, Glickman JN, Tschurtschenthaler M, Hartwig J, Hosomi S, *et al.* (2013). Paneth cells as a site of origin for intestinal inflammation. Nature 503, 272–276.

Ayabe T, Satchell DP, Wilson CL, Parks WC, Selsted ME, Ouellette AJ (2000). Secretion of microbicidal alpha-defensins by intestinal Paneth cells in response to bacteria. Nat Immunol 1, 113–118.

Baig MA, Qadir A, Rasheed J (2006). A review of eosinophilic gastroenteritis. J Nat Med Assoc 98, 1616–1619.

Baumgart M, Dogan B, Rishniw M, Weitzman G, Bosworth B, Yantiss R, Orsi RH, Wiedmann M, McDonough P, Kim SG, *et al.* (2007). Culture independent analysis of ileal mucosa reveals a selective increase in invasive Escherichia coli of novel phylogeny relative to depletion of Clostridiales in Crohn's disease involving the ileum. ISME J 1, 403–418.

Bertolotti A, Wang X, Novoa I, Jungreis R, Schlessinger K, Cho JH, West AB, Ron D (2001). Increased sensitivity to dextran sodium sulfate colitis in IRE1beta-deficient mice. J Clin Invest 107, 585–593.

Bevins CL, Salzman NH (2011). Paneth cells, antimicrobial peptides and maintenance of intestinal homeostasis. Nat Rev Microbiol 9, 356–368.

Cadwell K, Liu JY, Brown SL, Miyoshi H, Loh J, Lennerz JK, Kishi C, Kc W, Carrero JA, Hunt S, *et al.* (2008). A key role for autophagy and the autophagy gene Atg16l1 in mouse and human intestinal Paneth cells. Nature 456, 259–263.

Christianson JC, Olzmann JA, Shaler TA, Sowa ME, Bennett EJ, Richter CM, Tyler RE, Greenblatt EJ, Harper JW, Kopito RR (2012). Defining human ERAD networks through an integrative mapping strategy. Nat Cell Biol 14, 93–105.
Christianson JC, Ye Y (2014). Cleaning up in the endoplasmic reticulum: ubiquitin in charge. Nat Struct Mol Biol 21, 325–335.
Cohen SB, Denkers EY (2015). Impact of Toxoplasma gondii on dendritic cell subset function in the intestinal mucosa. J Immunol 195, 2754–2762.
Das I, Png CW, Oancea I, Hasnain SZ, Lourie R, Proctor M, Eri RD, Sheng Y, Crane DI, Florin TH, *et al.* (2013). Glucocorticoids alleviate intestinal ER stress by enhancing protein folding and degradation of misfolded proteins. J Exp Med 210, 1201–1216.
Dethlefsen L, Eckburg PB, Bik EM, Relman DA (2006). Assembly of the human intestinal microbiota. Trends Ecol Evol 21, 517–523.
Egan CE, Cohen SB, Denkers EY (2012). Insights into inflammatory bowel disease using Toxoplasma gondii as an infectious trigger. Immunol Cell Biol 90, 668–675.
Francisco AB, Singh R, Li S, Vani AK, Yang L, Munroe RJ, Diaferia G, Cardano M, Biunno I, Qi L, *et al.* (2010). Deficiency of suppressor enhancer lin12 1 like (SEL1L) in mice leads to systemic endoplasmic reticulum stress and embryonic lethality. J Biol Chem 285, 13694–13703.
Garner CD, Antonopoulos DA, Wagner B, Duhamel GE, Keresztes I, Ross DA, Young VB, Altier C (2009). Perturbation of the small intestine microbial ecology by streptomycin alters pathology in a Salmonella enterica serovar typhimurium murine model of infection. Infect Immun 77, 2691–2702.
Heazlewood CK, Cook MC, Eri R, Price GR, Tauro SB, Taupin D, Thornton DJ, Png CW, Crockford TL, Cornall RJ, *et al.* (2008). Aberrant mucin assembly in mice causes endoplasmic reticulum stress and spontaneous inflammation resembling ulcerative colitis. PLoS Med 5, e54.
Hetz C (2012). The unfolded protein response: controlling cell fate decisions under ER stress and beyond. Nat Rev Mol Cell Biol 13, 89–102.
Hoskins LC, Agustines M, McKee WB, Boulding ET, Kriaris M, Niedermeyer G (1985). Mucin degradation in human colon ecosystems. Isolation and properties of fecal strains that degrade ABH blood group antigens and oligosaccharides from mucin glycoproteins. J Clin Invest 75, 944–953.
Hoskins LC, Boulding ET (1981). Mucin degradation in human colon ecosystems. Evidence for the existence and role of bacterial subpopulations producing glycosidases as extracellular enzymes. J Clin Invest 67, 163–172.
Ji Y, Sun S, Goodrich JK, Kim H, Poole AC, Duhamel GE, Ley RE, Qi L (2014). Diet-induced alterations in gut microflora contribute to lethal pulmonary damage in TLR2/TLR4-deficient mice. Cell Rep 8, 137–149.
Joossens M, Huys G, Cnockaert M, De Preter V, Verbeke K, Rutgeerts P, Vandamme P, Vermeire S (2011). Dysbiosis of the faecal microbiota in patients with Crohn's disease and their unaffected relatives. Gut 60, 631–637.
Kaneko M, Yasui S, Niinuma Y, Arai K, Omura T, Okuma Y, Nomura Y (2007). A different pathway in the endoplasmic reticulum stress-induced expression of human HRD1 and SEL1 genes. FEBS Lett 581, 5355–5360.
Kaser A, Adolph TE, Blumberg RS (2013). The unfolded protein response and gastrointestinal disease. Semin Immunopathol 35, 307–319.
Kaser A, Lee AH, Franke A, Glickman JN, Zeissig S, Tilg H, Nieuwenhuis EE, Higgins DE, Schreiber S, Glimcher LH, Blumberg RS (2008). XBP1 links ER stress to intestinal inflammation and confers genetic risk for human inflammatory bowel disease. Cell 134, 743–756.
Liu TC, Gao F, McGovern DP, Stappenbeck TS (2014). Spatial and temporal stability of paneth cell phenotypes in Crohn's disease: implications for prognostic cellular biomarker development. Inflamm Bowel Dis 20, 646–651.
Namba T, Tanaka K, Ito Y, Ishihara T, Hoshino T, Gotoh T, Endo M, Sato K, Mizushima T (2009). Positive role of CCAAT/enhancer-binding protein homologous protein, a transcription factor involved in the endoplasmic reticulum stress response in the development of colitis. Am J Pathol 174, 1786–1798.
Niederreiter L, Fritz TM, Adolph TE, Krismer AM, Offner FA, Tschurtschenthaler M, Flak MB, Hosomi S, Tomczak MF, Kaneider NC, *et al.* (2013). ER stress transcription factor Xbp1 suppresses intestinal tumorigenesis and directs intestinal stem cells. J Exp Med 210, 2041–2056.
Ochoa R, Breitschwerdt EB, Lincoln KL (1984). Immunoproliferative small intestinal disease in Basenji dogs: morphologic observations. Am J Vet Res 45, 482–490.
Odze R (2003). Diagnostic problems and advances in inflammatory bowel disease. Mod Pathol 16, 347–358.
Olzmann JA, Kopito RR, Christianson JC (2013). The mammalian endoplasmic reticulum-associated degradation system. Cold Spring Harb Perspect Biol 5, a013185.
Park SW, Zhen G, Verhaeghe C, Nakagami Y, Nguyenvu LT, Barczak AJ, Killeen N, Erle DJ (2009). The protein disulfide isomerase AGR2 is essential for production of intestinal mucus. Proc Natl Acad Sci USA 106, 6950–6955.
Png CW, Linden SK, Gilshenan KS, Zoetendal EG, McSweeney CS, Sly LI, McGuckin MA, Florin TH (2010). Mucolytic bacteria with increased prevalence in IBD mucosa augment in vitro utilization of mucin by other bacteria. Am J Gastroenterol 105, 2420–2428.
Prindiville T, Cantrell M, Wilson KH (2004). Ribosomal DNA sequence analysis of mucosa-associated bacteria in Crohn's disease. Inflamm Bowel Dis 10, 824–833.
Qi L, Yang L, Chen H (2011). Detecting and quantitating physiological endoplasmic reticulum stress. Meth Enzymol 490, 137–146.
Sha H, He Y, Chen H, Wang C, Zenno A, Shi H, Yang X, Zhang X, Qi L (2009). The IRE1alpha-XBP1 pathway of the unfolded protein response is required for adipogenesis. Cell Metab 9, 556–564.
Sha H, Sun S, Francisco AB, Ehrhardt N, Xue Z, Liu L, Lawrence P, Mattijssen F, Guber RD, Panhwar MS, *et al.* (2014). The ER-associated degradation adaptor protein Sel1L regulates LPL secretion and lipid metabolism. Cell Metab 20, 458–470.
Sheng YH, Lourie R, Linden SK, Jeffery PL, Roche D, Tran TV, Png CW, Waterhouse N, Sutton P, Florin TH, McGuckin MA (2011). The MUC13 cell-surface mucin protects against intestinal inflammation by inhibiting epithelial cell apoptosis. Gut 60, 1661–1670.
Simpson KW, Dogan B, Rishniw M, Goldstein RE, Klaessig S, McDonough PL, German AJ, Yates RM, Russell DG, Johnson SE, *et al.* (2006). Adherent and invasive Escherichia coli is associated with granulomatous colitis in boxer dogs. Infect Immun 74, 4778–4792.
Sun S, Shi G, Han X, Francisco AB, Ji Y, Mendonca N, Liu X, Locasale JW, Simpson KW, Duhamel GE, *et al.* (2014). Sel1L is indispensable for mammalian endoplasmic reticulum-associated degradation, endoplasmic reticulum homeostasis, and survival. Proc Natl Acad Sci USA 111, E582–E591.
Sun S, Shi G, Sha H, Ji Y, Han X, Shu X, Ma H, Inoue T, Gao B, Kim H, *et al.* (2015). IRE1$\alpha$ is an endogenous substrate of endoplasmic reticulum-associated degradation. Nat Cell Biol 17, 1546–1555.
Travers KJ, Patil CK, Wodicka L, Lockhart DJ, Weissman JS, Walter P (2000). Functional and genomic analyses reveal an essential coordination between the unfolded protein response and ER-associated degradation. Cell 101, 249–258.
Tsuru A, Fujimoto N, Takahashi S, Saito M, Nakamura D, Iwano M, Iwawaki T, Kadokura H, Ron D, Kohno K (2013). Negative feedback by IRE1beta optimizes mucin production in goblet cells. Proc Natl Acad Sci USA 110, 2864–2869.
Vaishnava S, Behrendt CL, Ismail AS, Eckmann L, Hooper LV (2008). Paneth cells directly sense gut commensals and maintain homeostasis at the intestinal host-microbial interface. Proc Natl Acad Sci USA 105, 20858–20863.
VanDussen KL, Liu TC, Li D, Towfic F, Modiano N, Winter R, Haritunians T, Taylor KD, Dhall D, Targan SR, *et al.* (2014). Genetic variants synthesize to produce paneth cell phenotypes that define subtypes of Crohn's disease. Gastroenterology 146, 200–209.
Willing BP, Dicksved J, Halfvarson J, Andersson AF, Lucio M, Zheng Z, Jarnerot G, Tysk C, Jansson JK, Engstrand L (2010). A pyrosequencing study in twins shows that gastrointestinal microbial profiles vary with inflammatory bowel disease phenotypes. Gastroenterology 139, 1844–1854 e1841.
Wlodarska M, Kostic AD, Xavier RJ (2015). An integrative view of microbiome-host interactions in inflammatory bowel diseases. Cell Host Microbe 17, 577–591.
Yagishita N, Ohneda K, Amano T, Yamasaki S, Sugiura A, Tsuchimochi K, Shin H, Kawahara K, Ohneda O, Ohta T, *et al.* (2005). Essential role of synoviolin in embryogenesis. J Biol Chem 280, 7909–7916.
Yang L, Xue Z, He Y, Sun S, Chen H, Qi L (2010). A Phos-tag-based method reveals the extent of physiological endoplasmic reticulum stress. PLoS One 5, e11621.
Yoshida H, Matsui T, Hosokawa N, Kaufman RJ, Nagata K, Mori K (2003). A time-dependent phase shift in the mammalian unfolded protein response. Dev Cell 4, 265–271.
Zhang HS, Chen Y, Fan L, Xi QL, Wu GH, Li XX, Yuan TL, He SQ, Yu Y, Shao ML, *et al.* (2015). The endoplasmic reticulum stress sensor IRE1alpha in intestinal epithelial cells is essential for protecting against colitis. J Biol Chem 290, 15327–15336.
Zhao F, Edwards R, Dizon D, Afrasiabi K, Mastroianni JR, Geyfman M, Ouellette AJ, Andersen B, Lipkin SM (2010). Disruption of Paneth and goblet cell homeostasis and increased endoplasmic reticulum stress in Agr2-/- mice. Dev Biol 338, 270–279.